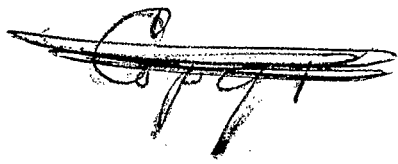

TECHNICAL MEMORANDUMS

NATIONAL ADVISORY COMMITTEE FOR AERONAUTICS

No. 752

ADDITIONAL TEST DATA ON STATIC LONGITUDINAL STABILITY

By Walter Hübner

Luftfahrtforschung
Vol. XI, No. 1, May 15, 1934

Washington
August 1934

NATIONAL ADVISORY COMMITTEE FOR AERONAUTICS

TECHNICAL MEMORANDUM NO. 752

ADDITIONAL TEST DATA ON STATIC LONGITUDINAL STABILITY*

By Walter Hübner

SUMMARY

1. In this particular airplane (Junkers F 13 ge) very minute changes in elevator displacement are equivalent to a profound change in lift. This "response" abates as the lift increases; it is not as pronounced at idling as it is with full throttle. For equal rapid up-elevator the case A accelerations with full throttle should exceed those at idling. Changing from idling to full throttle with elevator locked results in markedly higher lift. The increase in lift with the angle of attack is considerably greater with full throttle. Accelerations due to gusts will probably be greater with full throttle than at no load. With full throttle the static stability is lower despite the higher dynamic pressure on the tail surface and the apparently smaller downwash angle. This is largely due to the fact that the change of lift with the angle of stabilizer setting is greater with full throttle.

2. The stability with elevator released is about the same as with elevator locked when the c.g. of the elevator lies in its axis, but smaller with elevator released when the c.g. is ahead of the axis and greater with elevator locked when aft of the axis. An additional 13 pounds of weight in the elevator balance shifted the neutrally stable c.g. position from 40 to 30 percent of the mean chord with full throttle, and from 44 to 36 percent at idling. The effect of c.g. displacements of the elevator on the stability with elevator released is less with full throttle than at idling.

3. For equal equilibrium condition, the elevator forces are greater at idling than with full throttle. The ratio: equilibrium-dynamic pressure with engine idling to

*"Weitere Ergebnisse von Messungen der statischen Längsstabilität." Luftfahrtforschung, May 15, 1934, pp. 5-15.

equilibrium-dynamic pressure with full throttle for the same stabilizer setting changes with this setting. It drops as the airplane is more noseheavy - as the equilibrium-dynamic pressure with full throttle is greater. Balance weights ahead of the elevator axis may lower the elevator control forces quite considerably; at the same time this results in lowered static longitudinal stability with elevator released.

A. STABILITY WITH ELEVATOR LOCKED

The purpose of the investigation was to explore the influence of the weights of the controls on the stability with elevator released. The available test data (reference 1) were extended to stability with elevator locked. In this connection the study of the propeller effect seemed of vital importance.

Test Procedure

The airplane was a Junkers F 13 ge low-wing monoplane (fig. 1). The measurements: elevator deflections, dynamic pressure, pitching, altitude, and propeller r.p.m. were effected in steady level flight for different c.g. positions at idling, full throttle, and five intermediate throttle settings.

The results with full throttle were serviceable up to $c_a \sim 1.2$; at higher lift coefficients* the airplane could not be held in equilibrium long enough without moving the elevator. For idling and partially closed throttle the figures could only be evaluated to $c_a \sim 0.6$. Elevator flutter about its axis at low dynamic pressures within an amplitude as high as 1° made accurate evaluation of the record impossible.

Accuracy of the Measurements

The instrumental errors were estimated as follows:

---

*At $c_a \geq 1.2$ the airplane had a tendency to yaw without changing in bank, thus going into a sideslip. This caused a rapid drop in dynamic pressure and was followed by pitching about the axis of roll.

Measurement	Estimated error	Measurement	Estimated error
Elevator deflection	$\pm 0.2^{\circ}$	r.p.m.	± 20 r.p.m.
Dynamic pressure	± 3 kg/m^2	Stabilizer setting	$\pm 0.1^{\circ}$
Pitching	$\pm 1^{\circ}$	c.g. position	$\pm 0.5\%$ t_m
Rate of climb	± 0.5 m/s	flight load	± 5 kg

The degree of accuracy attained is small despite the little scattering of the test points. It suffices for estimating the loads on the airplane in order of magnitude and mutual relationship but not, however, for the numerical evaluation of the obtained absolute figures as, say, the results of wind-tunnel measurements.

NOTATION

c_{mH} coefficient of pitching moment (positive = noseheavy moment).

α (deg.), angle of attack of airplane = angle between thrust axis and flight path (positive = level off).

α_w (deg.), downwash angle = angle between flight path and mean air-stream direction at tail surface (positive equivalent to decrease in α).

β_H (deg.), elevator deflection. (See fig. 2.)

δ_H (deg.), stabilizer setting. (See fig. 2.)

λ, coefficient of advance of propeller = flight speed to tip speed.

$r\ \%\ t_m$, rear c.g. position.

$r_o\%\ t_m$, neutrally stable c.g. = rear position of c.g. at which static stability about axis of pitching is zero with elevator locked.

(kg/m $\times$0.204818=lb./sq.ft.) (m/s$\times$3.28083=ft./sec.)
(kg$\times$2.20462=lb.)

q kg/m², dynamic pressure.

q_S kg/m², mean dynamic pressure in slipstream on tail surface.

q_L kg/m², mean dynamic pressure on tail surface with engine idling

S kg, propeller thrust.

● denote full throttle; ○, idling; ◑, partially closed throttle; × + denote values deduced from calculations or from shape of curves.

RESULTS

Figure 2 illustrates a direct test record: lift coefficient and elevator deflection for different stabilizer settings. The results for different c.g. positions and partially closed throttles are similar. The curves obtained with full throttle are bent, a trend not recognized in previous measurements, being made at comparatively low static stability whereby the change in elevator setting and the curvature were less. The instrumental accuracy also was less in the previous experiments.

The r.p.m. for different throttle settings versus dynamic pressure, shown in figure 3, afford another example. These data, together with corresponding measurements, gave the coefficient of advance λ.

Pitching Moment and Static Stability

The coefficient of pitching moment c_{mH} and the static stability $\delta c_{mH}/\delta c_a$ may be determined for the individual operating conditions for which λ is variable, as well as for different constant λ. Figure 4 shows c_{mH} versus c_a for several constant λ with full throttle. It reveals the change in λ at full throttle resulting from changed lift. Between $c_a = 0.2$ and $c_a = 1.3$, $\lambda =$ 0.24 to 0.11. With engine idling, $\lambda = 0.38$ and 0.40; that is, the changes are minute. For constant λ the de-

pendence of c_{mH} and c_a is in fairly linear relation; with full throttle the change in λ causes a curved change in c_{mH} in the sense of lowering the stability $\delta c_{mH}/\delta c_a$. The method of plotting figure 4 is that of the Göttingen Aerodynamic Institute and seems suitable for wind-tunnel and flight tests (reference 2).

Figure 5 shows the neutrally stable c.g. position r_o and the static elevator effect of $dc_{mH}/d\beta_H$ versus λ (mean q_s versus λ). As λ increases, r_o shifts to the rear, and $dc_{mH}/d\beta_H$ decreases rapidly. The ratio $dc_{mH}/d\beta_H$ in the slipstream to that in the undisturbed air stream is approximately equal to the ratio of the corresponding q_s/q. This ratio was obtained under the assumption that $dc_{mH}/d\beta_H$ and q at idling, amount to 85 and 90 percent of the value for the undisturbed air stream.

TABLE I

λ = propeller advance	c_a = lift coefficient	$\frac{dc_{mH}}{d\beta_H}$	r_o = c.g. position for $\frac{dc_{mH}}{dc_a} = 0$
0.109	1.3	0.035	
0.114	1.2	0.0337	
0.118	1.1	0.031	
0.124	1.0	0.030	
0.130	0.9	0.0275	
0.138	0.8	0.0255	
0.146	0.7	0.0236	
0.156	0.6	0.0228	
0.168	0.5	0.022	
0.15	0.66	0.0242	0.374
0.20	0.32	0.0194 (0.02*)	0.376 (0.365*)
0.25	-	0.0165	0.376
0.30	-	0.0148	0.38
0.35	-	0.0142	0.387
0.40	-	0.0138 (0.014*)	0.3915 (0.39*)

*Previous measurements (reference 1).

Static Elevator Effect $\frac{\delta c_{mH}}{\delta \beta_H}$ and Dynamic Pressure at Tail Surface

The value of $\delta c_{mH}/\delta \beta_H$ with full throttle and engine idling, as given in previous reports, was determined for different λ (fig. 5) and with full throttle for different c_a (fig. 6).

It will be seen that the elevator effectiveness increases as λ decreases and c_a increases. These changes are substantially stipulated by the changed dynamic pressure in the slipstream. On the premise of the mean dynamic pressure on the tail at idling being 85 and 90 percent of the dynamic pressure q (reference 3), which gives the mean dynamic pressure on the tail surface in a glide at ~ 90 percent of the dynamic pressure based on wind-tunnel data) we computed q_S/q_L (figs. 5 and 6).

Then we determined from q_S the propeller thrust which would result conformably to the jet theory under the assumption that the jet section on the tail surface equals the propeller disk area. A comparison with dynamometer hub test data shows the actual thrust to be about 60 percent higher than that thus determined (fig. 7). This discrepancy may in part be due to the fact that the jet section at the tail surface is (about 60 percent) greater than the propeller disk area.

The Relation of Air Load to Angle of Attack

The angle of attack is the difference between angle of climb and pitch; that is, of two factors not amenable to very exact determination. The first is particularly difficult to define because of the great errors in the rate-of-climb measurement. The results obtained for the angle of attack (fig. 8) are therefore only approximate. However, the data agree quite closely with previous measurements.

According to figure 8, the rise of c_a against the angle of attack with full throttle is $\delta\alpha/\delta c_a \sim 9^\circ$, on account of the changes in λ; that is, greater than corresponds to the aspect ratio of the wing for constant λ.

The dependence of the air loads on the tail surface may be estimated conformably to figure 9 (obtained from

measurements with different stabilizer settings) as follows:

$$\frac{dc_{mH}}{d\alpha} = \frac{dc_{mH}}{d\delta_H} \sim 1.48 \times \frac{dc_{mH}}{d\beta_H}.$$

Mean Downwash Angle on Tail Surface

On the basis of the test data the mean downwash angle at idling and full throttle and its dependence on the lift can be estimated.

The moment due to propeller thrust may be ignored, since here the thrust line passes approximately through the c.g. of the airplane. Since α and δ_H are known, the tail surface moment without downwash effect is determinable. For $c_a = 0$, the difference of total moment and tail-surface moment gives the wing moment $c_{m0} \sim 0.10$. The stability of the wing was assumed at $\delta c_{mH}/\delta c_a = 0.25$ for $r = 0$, that is, c.g. position in leading edge of center section of wing. The difference of total moment and wing moment gives the tail surface moment without downwash effect. The difference of tail-surface moments with and without downwash gives the moments c_{mW} due to downwash. The downwash angle results from the moment:

$$\alpha_w = \frac{c_{mW}\, d\alpha_H}{dc_{mH}}$$

Figure 10 illustrates the individual effects on the moment curve with full throttle (relative to the leading edge of the mean wing chord). It was assumed that c_{m0} = constant for the wing moment and $dc_m = 0.25$ and that the downwash angle $\alpha_w = 0$ at $c_a = 0$. From figures 6 and 9 we computed $dc_{mH}/d\alpha$ and from it the tail-surface moment without downwash by means of the angle-of-attack measurements. The sum of this moment and that of the wing gives the total moment without downwash effect. The moment produced by the downwash is given by the difference between the total moments with and without downwash effect. (For the latter, see fig. 4.) The downwash angle α_w results from dividing this "downwash moment" by $dc_{mH}/d\alpha$. On the premise of zero downwash at $c_a = 0$, we have $c_{m0} \sim 0.10$. Figure 11 shows the discussed downwash angle α_w versus c_a, as determined for full throttle and idling conforma-

bly to the assumptions cited in figure 10. These downwash angles are greater at idling than with full throttle. The explanation for this is that the slipstream pushes the flow at the tail surface more toward the propeller axis. If this holds true, it should be possible to influence the stability through the setting of the propeller axis.

On the other hand, it is questionable whether the assumption c_{m0} = constant is legitimate for full throttle flight. It is not improbable that c_{m0} changes with λ. In this particular airplane the slipstream lies substantially on the upper surface of the center section of the wing. Hence the higher dynamic pressure on the upper side with full throttle; this increment is so much greater as the lift coefficient is greater and as λ is smaller. A greater circulation, i.e., lift, is therefore to be expected. This rise in c_a may perhaps be bound up with a greater c_{m0} (analogy with changed camber). But, if c_{m0} increases while λ decreases, the downwash angles with full throttle must be greater than those obtained on the premise of c_{m0} = constant.

B. EFFECT OF MOMENTS OF WEIGHT OF CONTROLS ON THE PITCHING MOMENT WITH ELEVATOR RELEASED

Previous flight tests (reference 4) had shown the longitudinal stability with elevator released to be greater at any c.g. position than with elevator locked. This was attributed to the influence of the unbalanced weight of the controls and to the elevator and theoretically affirmed by Blenk (reference 5). However, a check against free flight measurements seemed very opportune.

Test Procedure

The same Junkers F 13 ge was used again. The test program included three different control weight arrangements with which the equilibrium dynamic pressure for elevator released was measured in dependence of stabilizer setting and of c.g. position with full throttle and engine idling. The wing loading was around 40 kg/m^2.

NOTATION

c_{mH}, pitching moment coefficient relative to leading edge of mean wing chord (positive = noseheavy moment).

β_H (deg.), elevator deflection (positive = up elevator).

μ_H (deg.), control stick displacement (positive = pulling).

δ_H (deg.), stabilizer setting relative to thrust axis (positive when leading edge of stabilizer is below propeller axis).

ϑ_H (deg.), pitch of airplane = angle between thrust axis and horizon (positive in climb).

P_G (kg), control stick force due to control weight moments (positive when direction of force is as with noseheavy airplane).

t_m (m), mean wing chord = chord at $2b/3\pi$ from center of wing = 2.62 m.

t_{Rm} (m), mean elevator chord = 0.57 m.

Results of Tests

Figures 12 and 13 show the general experimental arrangements. The flight tests were made as follows (see table II):

Arrangement A.- A 6 kg weight placed at 0.41 m forward of elevator axis for balance; c.g. at -6.35 percent of mean elevator chord.

Arrangement B.- A 3 kg weight placed 0.42 m ahead of elevator axis for balance; c.g. at +3.4 percent of mean elevator chord.

Arrangement C.- No weights for elevator axis; a 3.7 kg weight on control stick; c.g. at 17.2 percent of mean elevator chord. (Previous measurements of elevator locked were made with this set-up - section A of this report.)

(m × 39.37 = in.)

Figure 14 shows the theoretical and experimental arrangement of control stick and elevator displacements together with the change in control transmission ratio with the elevator displacement.

The moments of the weight of the controls about the control lever axis were analytically defined according to individual weighing, as well as measured direct with a control force recorder. The results - the force on the control stick - are illustrated in figure 15 for divers elevator displacements versus angle of pitch of the airplane. The dependence of pitch and lift coefficient is seen in figure 16, while the relations between elevator displacement, stabilizer setting, and c.g. position are known from section A of this report.

Pitching Moments with Elevator Locked, and Released

The pitching moment coefficient in figures 17, 18, 20, and 21 are referred to the leading edge of the mean wing chord, and computed for a stabilizer setting $\delta_H = -2.5^\circ$ with elevator locked and extrapolated for elevator setting $\beta_H = 0$. In view of the number and scattering of the test points, table II gives only a few mean values.

The setting, with elevator released, differs for each arrangement (figs. 19 and 22).*

With arrangement A this elevator displacement has the direction "up-elevator"; thus reducing the pitching moments. At idling the elevator displacement in "pulling" direction increases with the lift (see fig. 22), followed by a perceptible decrease in stability within the whole lift range explored. (See fig. 21.) With full throttle the elevator displacement changes little at higher c_a (see fig. 19), and only up to $c_a \sim 0.4$ may the change and reduction in stability be perceived. (See fig. 18.)

---

*No measurable effect of the c.g. position on these elevator displacements was obtainable within the explored range ($r \sim 27.8$ to 37 percent t_m). Consequently the conversion of the moment coefficients to other c.g. positions - at least, within this same range - appears justified.

TABLE II

Mean Values of Recorded Pitching Moment Coefficients

Relative to Leading Edge of Mean Wing Chord $\delta_H = -2.5^\circ$

c_a	c_m Elevator released $\beta_H=0^\circ$	c_m Elevator released Set-up A	c_m Elevator released Set-up B	c_m Elevator released Set-up C
Full throttle				
0.2	(0.035)	0.03	0.045	0.055
0.3	0.07	0.065	0.085	0.095
0.4	0.105	0.10	0.12	0.135
0.5	0.135	0.13	0.16	0.175
0.6	0.17	0.16	0.195	0.215
0.7	0.20	0.19	0.23	0.255
0.8	0.235	0.225	0.27	
0.9	0.265	0.26		
1.0	0.30	0.29		
1.1	0.33	0.32		
1.2	0.36	0.355		
Idling				
0.2	(0.045)	0.04	0.05	0.06
0.3	0.08	0.08	0.09	0.105
0.4	0.12	0.115	0.135	(0.15)
0.5	0.16	0.15	0.175	
0.6	0.20	0.185	0.215	

With arrangements B and C the c.g. of the elevator is aft of the axis, so with elevator released it assumes a "down-elevator" direction, which increases with the lift coefficient. The result is an increase in noseheavy moments with the lift in the sense of increased stability. The increment of the elevator deflection in "push" direction and through it of the stability, is greater for arrangement C than for B. Figure 23 depicts dc_m/dc_a versus c.g. position from the axis of the control with elevator released. (dc_m/dc_a is referred to the leading edge of the mean wing chord.) If the c.g. lies ahead of the hinge the stability with elevator released becomes less; if aft of the hinge, greater than with elevator locked.

A shift of the elevator c.g. of 10 percent of the mean elevator chord suffices, as may be seen, to shift the neutrally stable c.g. with full throttle from 1.5 to 3.5 percent, and from 2.5 to 4.5 percent of the mean wing chord at idling. It should be noted that arrangements A to C are not only unlike as to c.g. position but also as to weight of control.

The method of representation of figure 23 was chosen even though the unbalanced moment of the whole control is decisive for the control setting and the magnitude of the stability. Thus figure 23 and table II approximate the neutral stability of the airplane as to c.g. position relative to mean wing chord.*

TABLE III

Stability $\frac{dc_m}{dc_a}$ for the Different Arrangements**

Set-up	Balance weight kg	Moment about elevator hinge m kg	Weight of elevator kg	Distance of c.g. of elevator from hinge m	Distance of c.g. of elevator from hinge % of t_m	$\frac{dc_m}{dc_a}$ at $c_a \sim 0.3$ full throttle	$\frac{dc_m}{dc_a}$ at $c_a \sim 0.3$ idling
A	6	-0.82	22.7	-0.036	- 6.35	0.34	0.36
B	3	+0.38	19.7	+0.019	+ 3.4	0.375	0.405
C	0	+1.64	16.7	+0.098	+17.2	0.40	0.44
elevator locked	-	-	-	-	-	0.36	0.39

Arrangement	$\frac{dc_m}{dc_a}$ full throttle	$\frac{dc_m}{dc_a}$ idling	Reference
C	0.43	0.44	DVL Report No. 166 (reference 4)
Elevator locked	0.365	0.39	

*To illustrate: $dc_m/dc_a = 0.34$ (referred to leading edge of t_m) denotes that the airplane becomes neutrally stable at a c.g. position of 0.34 of the mean wing chord.

**Previous measurements yielded.

C. EFFECT OF c.g. POSITION OF ELEVATOR ON THE ELEVATOR CONTROL FORCES

The amount of the elevator force, that is, its rise with dynamic pressure changes, is dependent on the moments about the elevator axis as well as those of the weight of the controls. For this reason it seemed interesting to establish the manner in which changes in control moments affect the control force, that is, determine the elevator force in unaccelerated flight relative to the stabilizer setting for different control moment arrangements.

Test Procedure

The airplane was a Junkers F 13 ge (fig. 1). Its c.g. was at 28 percent of the mean wing chord with an approximate loading of 40 kg/m^2. The measurements included both full throttle and idling with different stabilizer settings. The control moment arrangements obtained with different weights in the elevator balance were as follows.

Arrangement	Balance weight kg	Moment about elevator axis m kg	Weight of elevator kg	Distance of c.g. from axis	
				m	% of mean elevator chord
A	6	-0.82	22.7	-0.036	-6.35
B	3	+0.38	19.7	+0.019	+3.4

NOTATION

c_{mH}*, pitching moment coefficient with elevator released relative to airplane c.g. (positive = noseheavy moment).

c_a, lift coefficient.

c_a*, lift coefficient at equilibrium with elevator released.

β_H (deg.), elevator displacement (up-elevator positive).

δ_H (deg.), stabilizer setting (positive when leading edge of stabilizer is below axis of propeller).

P_H (kg), elevator control force = force on control stick necessary to hold airplane in equilibrium (positive when force is as with noseheavy airplane).

q (kg/m^2), dynamic pressure.

q_V^* (kg/m^2), dynamic pressure at equilibrium with elevator released ($P = 0$), full throttle.

q_L^* (kg/m^2), dynamic pressure at equilibrium with elevator released ($P = 0$), idling.

Results of Tests

Effect of Stabilizer Setting on Elevator Control Force

The elevator control force and the corresponding displacements with arrangement A are shown in figures 24 and 25 versus the dynamic pressure for four stabilizer settings, and those with arrangement B for five stabilizer settings in figure 26. In the latter the elevator displacements have been omitted since they are not affected by a change in control moments; that is, correspond to those measured with arrangement A. These graphs show that a change in stabilizer setting modifies the equilibrium dynamic pressure q^* ($P = 0$) as well as the increase of the control force against dynamic pressure dP_H/dq. The trend of the control force is rectilinear up to small dynamic pressures, hence may be expressed for each stabilizer setting within the most important flight range by a value dP_H/dq. High absolute dP_H/dq denote that great control force must be applied to change the dynamic pressure without modifying the stabilizer setting. The test data reveal that dP_H/dq is great when the equilibrium dynamic pressure is low, that is, when, owing to small negative stabilizer settings, the airplane is tailheavy. On the other hand, if the airplane is noseheavy with the same c.g. position, then dP_H/dq is small; that is, less additional control force is needed to insure the same dynamic pressure changes.

To illustrate: With arrangement A for a stabilizer setting $\delta_H = -1.8^\circ$ at full throttle, it requires an 0.7 kg change in control force to raise or lower the dynamic pressure 10 kg/m^2, whereas for $\delta_H = -2.9^\circ$, it requires scarcely half as much (0.3 kg). With tailheavy stabilizer setting the control forces will probably be estimated as great; with noseheavy setting as small.

The rise of dP_H/dq is shown in figure 27, with c_a as ordinate resulting from equilibrium dynamic pressure q^* (table IV). The graphs show a straight line with full throttle and idling, which pass through the origin of the ordinate; consequently, dP_H/dq drops linearly with c_a^*. For equal c_a^*, dP_H/dq is greater at idling than with full throttle.

Comparison of Control Forces at Different c.g. Locations of the Elevator

According to figure 27, the differences of dP_H/dq with full throttle and engine idling are about the same for equal c_a^* with either arrangement, A or B. But the absolute values of dP_H/dq are markedly higher for B than for A. This means that shifting the c.g. of the elevator to the rear results in a substantial rise of control force.

Previous tests (reference 4) had shown that with constant equilibrium attitude (q^* and c_a^*) the value dP_H/dq changes linearly with the stability for elevator released dc_{mH}^*/dc_a, and becomes zero with it. Now for equal c.g. position with set-up A, the stability with free elevator is lower than with B, so that for this reason alone a smaller dP_H/dq may be expected.

For equal stabilizer setting dP_H/dq is about the same for both arrangements A and B. (See fig. 29.)

TABLE IV

Relation between Equilibrium Dynamic Pressure and Rise of Control Force with Stabilizer Setting

Control arrangement	δ_H	Full throttle			Engine idling			$\frac{q_L}{q_v}$	$q_L^*-q_v^*$
		Dynamic pressure at equilibrium q_v^* kg/m²	c_a^*	$\frac{dP_H}{dq}$	Dynamic pressure at equilibrium q_L^* kg/m²	c_a^*	$\frac{dP_H}{dq}$		kg/m²
A	-1.8	33	1.22	-0.073	70	0.575	-0.069	2.12	37
	-2.0	35	1.15	-0.064	79	0.51	-0.062	2.26	44
	-2.7	66	0.61	-0.039	108	0.375	-0.046	1.64	42
	-2.9	87	0.465	-0.03	132	0.305	-0.034	1.52	45
	-2.0	36	1.14		77.5	0.52		2.15	41.5
	-2.05	36.5	1.1		82	0.495		2.24	45.5
	-2.3	43.5	1.93		84	0.48		1.93	40.5
	-2.4	55	0.735		97	0.415		1.76	42
	-2.47	57			100			1.75	43
	-2.67	67	0.60		111	0.365		1.66	44
	-3.0	101			149			1.47	48
	-3.2	139			-			-	
B	-1.0	50	0.80	-0.108	86	0.465	-0.088	1.72	36
	-1.6	65	0.615	-0.076	104	0.385	-0	1.6	39
	-2.3	110	0.365	-0.05	152	0.265	-0.052	1.38	42
	-2.6	145	0.275	-0.038	178	0.225	-0.044	1.23	33
	-2.9	204	0.20	-0.030	240	0.17	-0.034	1.17	36
	-1.6				113	0.35			
	-1.6				111.5	0.36			
	-2.16	105.5	0.38						
	-2.16	111.5	0.36		134	0.30		1.2	22.5
	-2.16	110	0.36						
	-2.6	151	0.26						

Effect of Stabilizer Setting and Elevator c.g. Location on the Equilibrium Dynamic Pressure for Full Throttle and Idling

This relationship is shown in figure 28. It is also seen how the equilibrium dynamic pressure changes when changing from full throttle to idling without modifying the stabilizer setting. This change should be small. (According to Airplane Specifications Bulletin No. 4515, "The airplane speed with throttling ..... shall not exceed 20 percent of the level-flight speed with full throttle.") For comparison, we give in figure 30, q_L^*/q_v^*; that is, the ratio of equilibrium dynamic pressure at idling and full throttle for equal stabilizer setting versus full throttle dynamic pressure q_v^*. This ratio is great at low q_v^* and decreases rapidly with increasing q_v^*.

Bringing the airplane with full throttle at low dynamic pressure into equilibrium and then throttling the engine down to idling, results in a new equilibrium dynamic pressure which is more than twice as high as the original. Contrariwise, the dynamic pressure at idling is only about 20 percent higher than with full throttle when the latter was chosen high. Table IV shows that the difference $(q_L^* - q_v^*)$ is of the same order of magnitude for any stabilizer setting.

A comparison of q_L^*/q_v^* with either control arrangement (see fig. 30 and table IV) shows that arrangement B is somewhat more propitious than A, although the difference is slight.

Translation by J. Vanier,
National Advisory Committee
for Aeronautics.

REFERENCES

1. Hübner, W.: Ergebnisse von Messungen der Stabilität um die Querachse. DVL Yearbook, 1931, p. 684.

2. Untersuchungen einiger Flugzeugmodelle: e) Flugzeugmodell mit Propeller, Ergebnisse der Aerodynamischen Versuchsanstalt zu Göttingen, vol. III, p. 125.

3. Gorsky, V. P.: Untersuchung über den Einfluss Flugzeuges. Central Aero-Hydrodynamical Institute, Russia, vol. 131.

4. Hübner, W.: Messung der Höhensteuerkräfte und der Längsstabilität eines Flugzeuges vom Muster Junkers F 13 ge. DVL Yearbook, 1930, p. 638

5. Blenk, H.: Über die Längsstabilität eines Flugzeuges mit losgelassenem Höhensteuer. DVL Yearbook, 1930, p. 61.

LEGENDS

FIGURE 1.-General arrangement drawing of Junkers F 13 ge.

Characteristics

F,	wing area	44.4 m^2 (477.92 sq.ft.)
b,	span	17.75 m (58.23 ft.)
t_m,	mean chord (at $2b/2\pi$ of wing center)	2.62 m (8.60 ft.)
a,	rear position of leading edge of mean wing chord from leading edge of center section of wing	0.518 m (.518 ft.)
F_H,	area of horizontal tail surfaces	7.0 m (22.97 ft.)
b_H,	span of horizontal tail surfaces	5.6 m (18.37 ft.)
Δ_H,	width of fuselage at leading edge of stabilizer	0.4 m (1.31 ft.)
$b_H - \Delta_H$,	free span-width of horizontal tail surfaces	5.2 m (17.06 ft.)
$\lambda_H = b_H^2/F_H$,	aspect ratio of horizontal tail surfaces	4.5
$\lambda_H=(b_H-\Delta_H)^2/F_H$,	aspect ratio of horizontal tail surface	3.9
F_F,	area of stabilizer	3.67 m^2 (39.5 sq.ft.)
F_R,	area of elevator	3.33 m^2 (35.84 sq.ft.)
F_R/F_H,	relative area of elevator	0.475

H,	distance of elevator axis from c.g. of airplane	6.7 m (21.98 ft.)
Ft_m/l_H F_H,		2.48 m (8.14 ft.)
G_R,	net weight	1440.00 kg (3174.65 lb.)
G,	flight load	2300.00 kg (5070.63 lb.)
Engine,	Junkers L 5	
N,	horsepower	300.00 hp (295.89 hp.)
c.g. positions of operating range in % t_m,		~27.8 to 39.1

FIGURE 2.-c_a versus β_H for different stabilizer settings δ_H.

FIGURE 3.-Propeller r.p.m. versus dynamic pressure for different throttle settings.

FIGURE 4.-Moment coefficient c_{mH} versus c_a for different λ.

FIGURE 5.-c.g. position r_o and static elevator effect $dc_{mH}/d\beta_H$ versus λ.

FIGURE 6.-$dc_{mH}/d\beta_H$ and q_L versus c_a.

FIGURE 7.-Comparison of propeller thrust computed from q_S with thrust test data.

FIGURE 8.-c_a versus α.

FIGURE 9.-Elevator displacement at zero lift versus stabilizer setting.

FIGURE 10.-Individual effects on c_m with full throttle.

FIGURE 11.-Downwash angle α_w versus c_a.

FIGURE 12.-Control arrangement of Junkers F 13 ge.

FIGURE 13.-Elevator of Junkers F 13 ge.
Stabilizer area: 3.67 m^2 (39.5 sq.ft.).
Mean elevator chord: 0.57 m^2 (6.14 sq.ft.).
Elevator area: 3.33 m^2 (35.84 sq.ft.).

FIGURE 14.-Elevator and control stick displacement control transmission ratio ($\delta = 0^\circ$).

FIGURE 15.-Forces on control stick P_G caused by the moments of the weight of the controls with the three set-ups A, B, C. (Noseheavy moments positive ($\delta = 0^\circ$).)

FIGURE 16.-c_a versus pitch ϑ.

FIGURE 17.-Pitching moment coefficient c_m versus leading edge of mean wing chord for elevator locked with full throttle ($\delta = -2.5^\circ$, $\beta_H = 0$).

FIGURE 18.-Pitching moment coefficient c_m versus leading edge of mean wing chord for elevator released with full throttle ($\delta = -2.5^\circ$, $\beta_H = 0$).

FIGURE 19.-Elevator displacement β_H with elevator released with full throttle for set-ups A to C.

FIGURE 20.-Pitching moment coefficient for elevator locked at idling ($\delta = -2.5^\circ$, $\beta_H = 0$).

FIGURE 21.-Pitching moment coefficient for elevator released at idling ($\delta = -2.5^\circ$, $\beta_H = 0$).

FIGURE 22.-Displacement β_H with elevator released at idling for set-ups A to C.

FIGURE 23.-Effect of c.g. position of elevator on dc_m/dc_a with elevator released.

FIGURE 24.-Arrangement A. Elevator displacement and control force at $\delta_H = -1.8^\circ$ and -2.0°.

FIGURE 25.-Arrangement A. Elevator displacement and stick force at $\delta_H = -2.7^\circ$ and -2.9°.

FIGURE 26.-Arrangement B. Control force at $\delta_H = -1.0^\circ$, -1.6°, -2.3°, -2.6°, and -2.9°.

FIGURE 27.-Relation between increase of control force $\frac{dP_H}{dq}$ and equilibrium attitude with free elevator $c_a^* \frac{dP_H}{dq}$ rises linearly with c_a^*, is greater at idling than with full throttle and greater with more rearward c.g. (arrangement B) than with more forward c.g. position (arrangement A).

FIGURE 28.-Equilibrium dynamic pressure and stabilizer setting with arrangements A and B.

FIGURE 29.-Increase of control force $\frac{dP_H}{dq}$ versus stabilizer setting.

FIGURE 30.- $\frac{q_L^*}{q_V^*}$ versus $q_V \frac{q_L^*}{q_V^*}$.

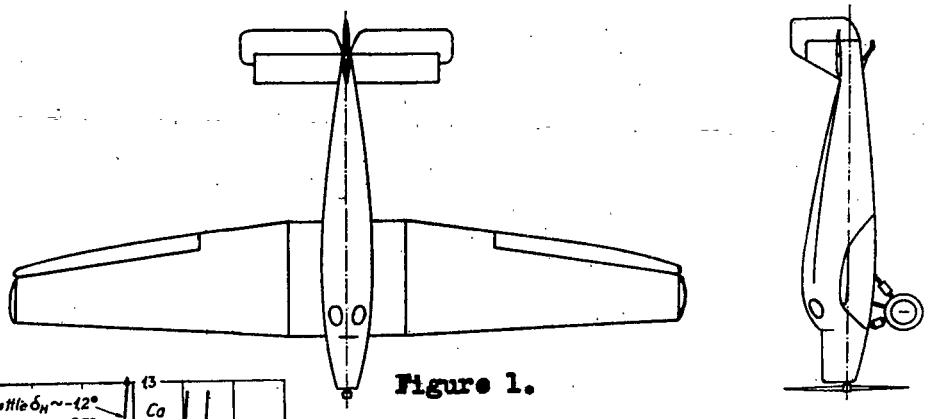

Figure 1.

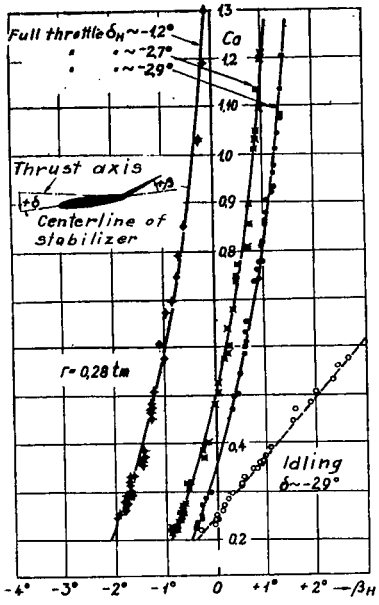

Figure 2.

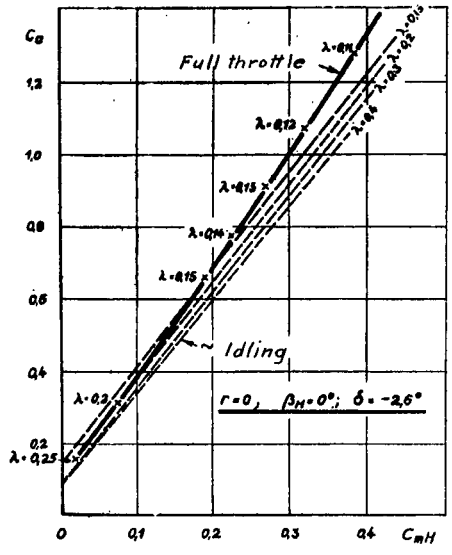

Figure 4.

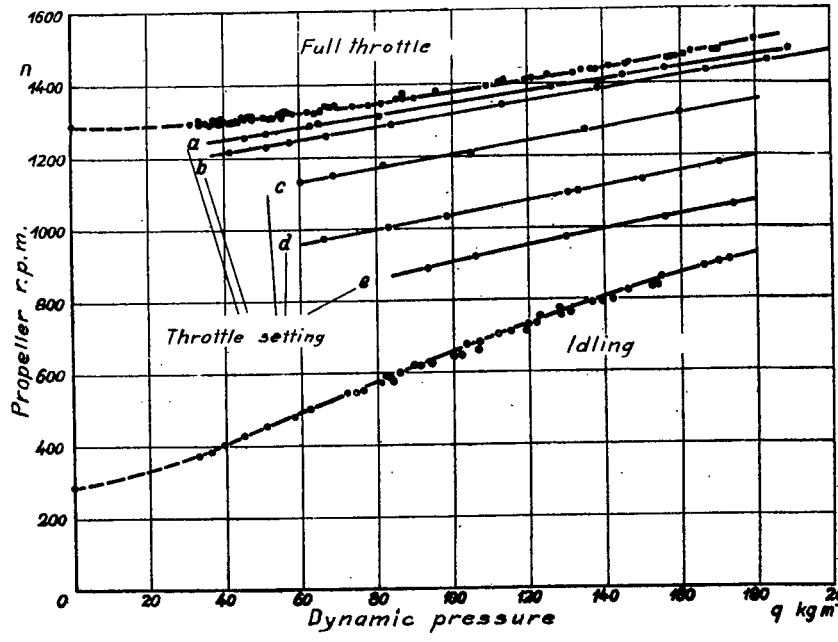

Figure 3.

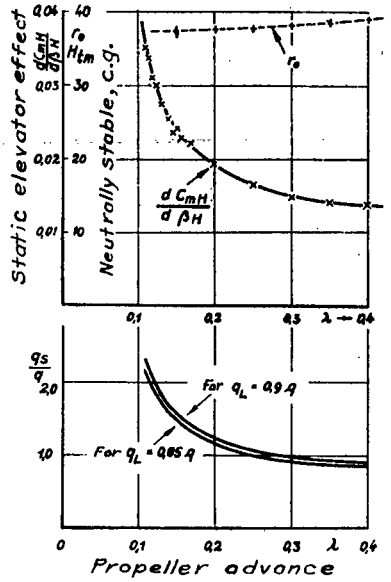

Figure 5.

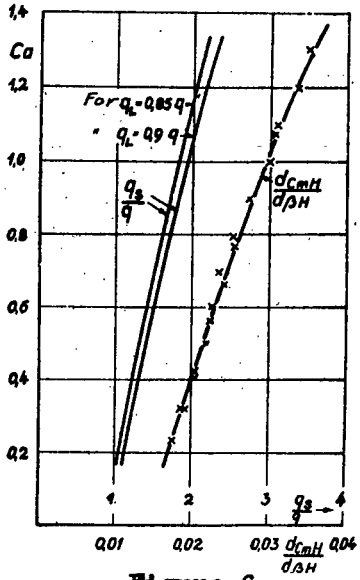

Figure 6.

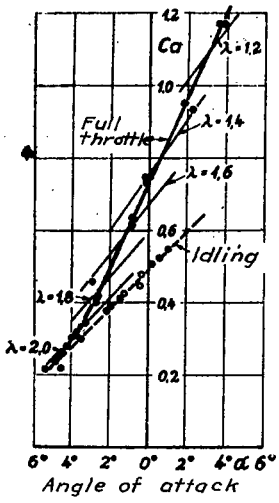

Figure 8.

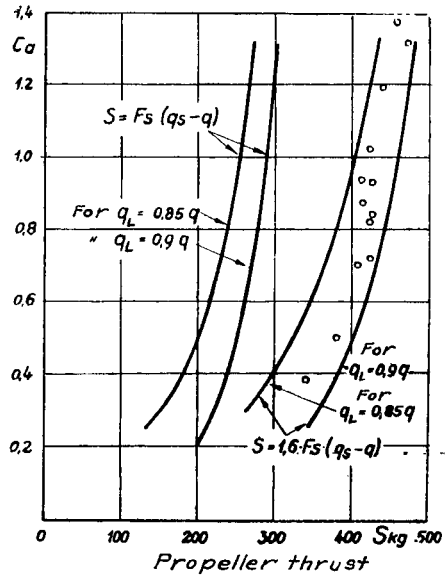

Figure 7.

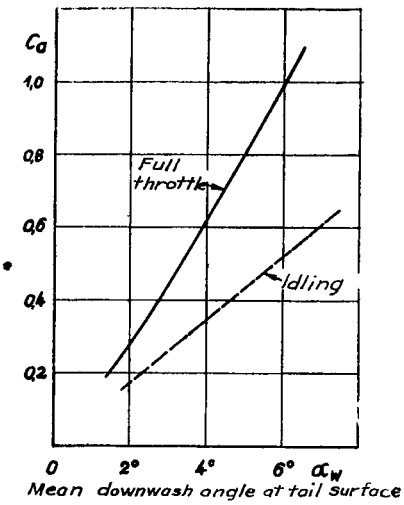

Figure 11.

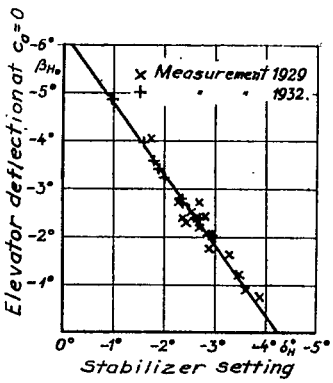

Figure 9.

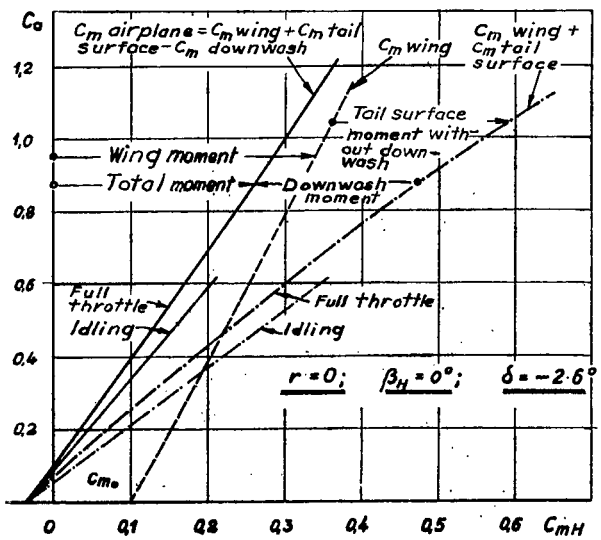

Figure 10.

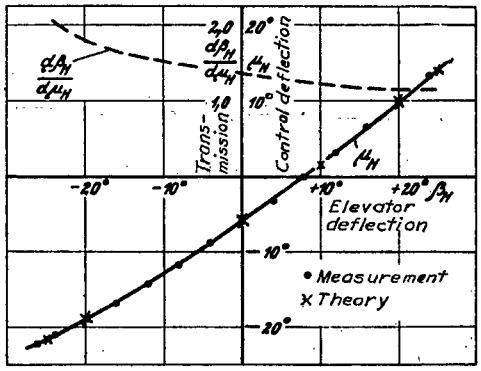

Figure 14.

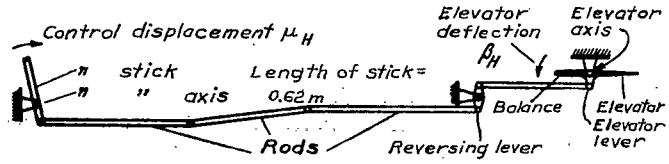

Figure 12.

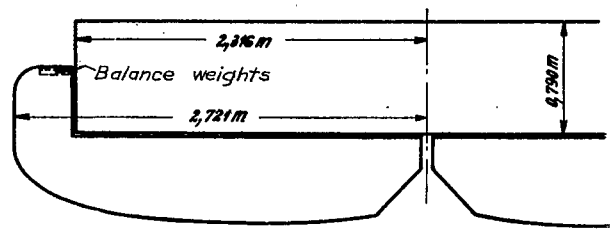

Figure 13.

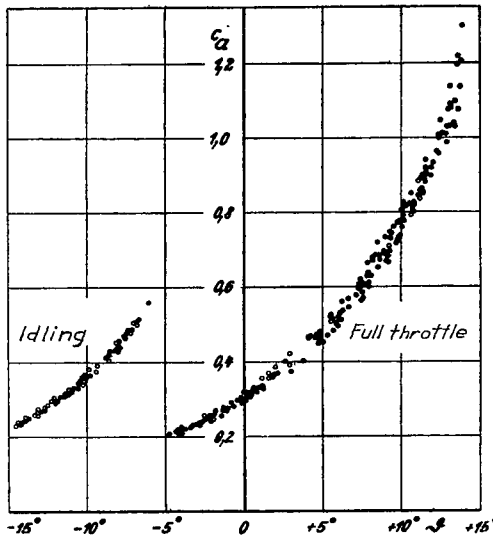

Figure 16.

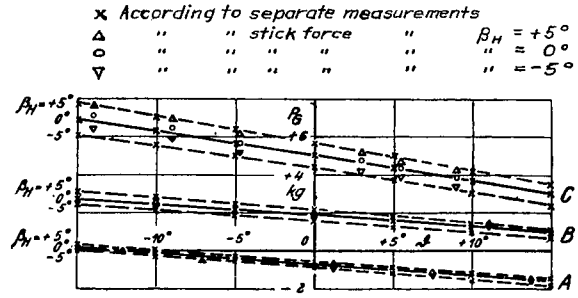

Figure 15.

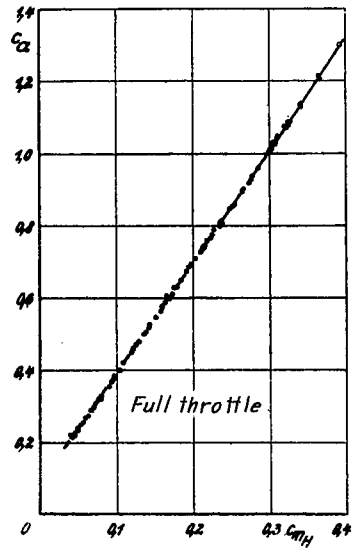

Figure 17.

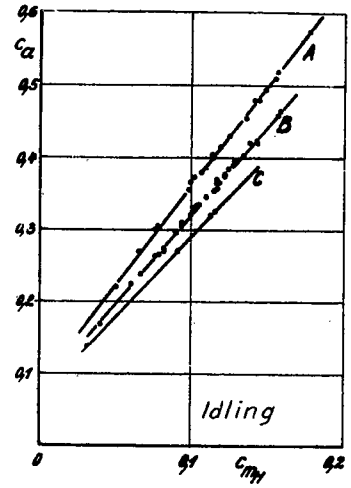

Figure 18.

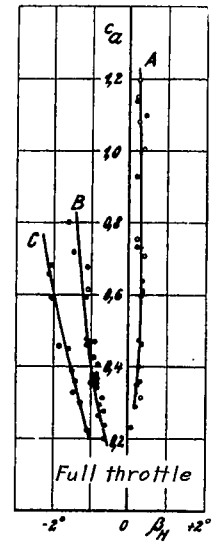

Figure 19.

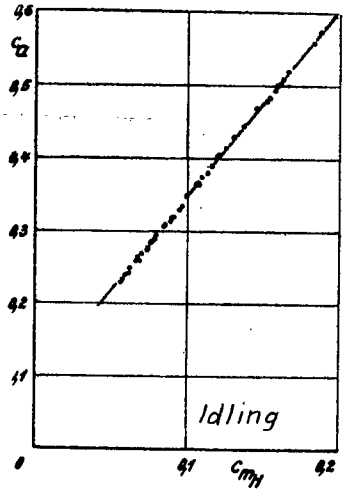

Figure 20.

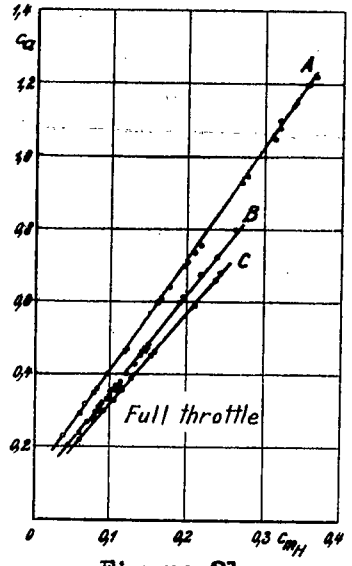

Figure 21.

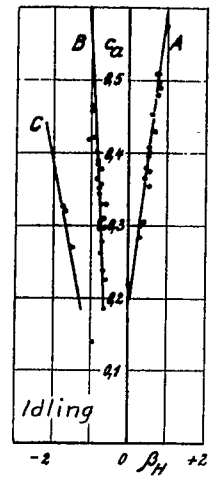

Figure 22.

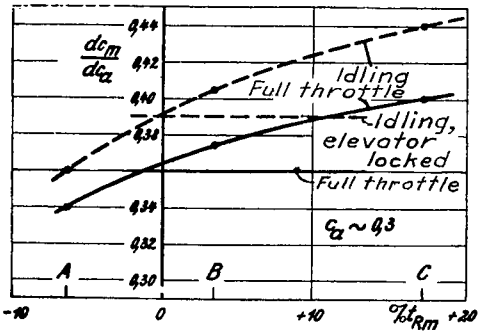

Figure 23.

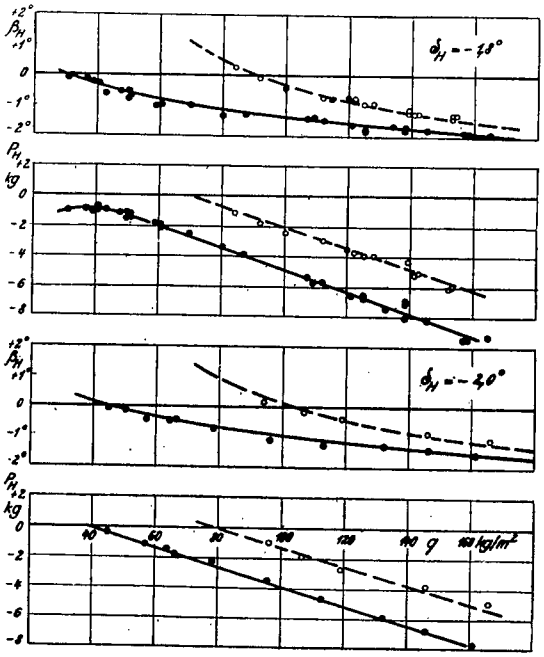

Figure 24.

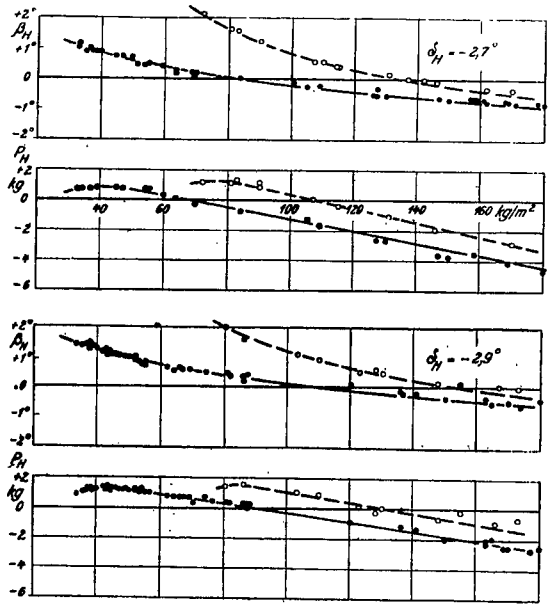

Figure 25.

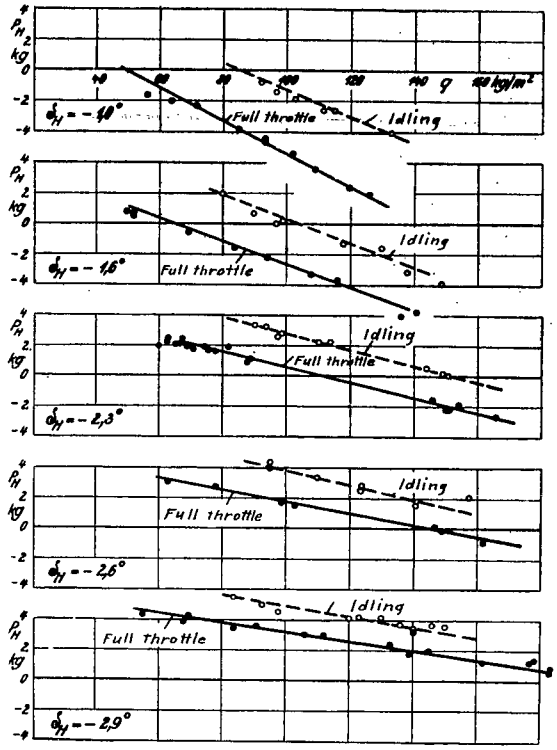

Figure 26.

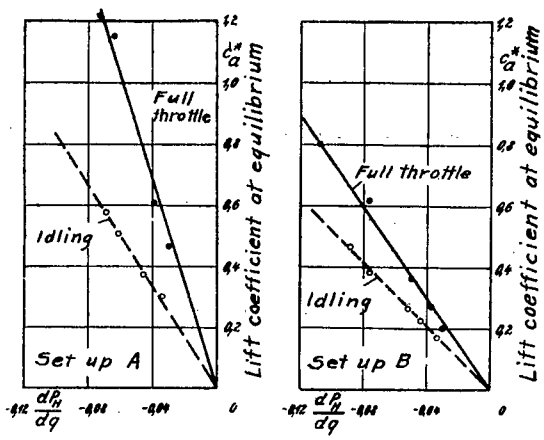

Figure 27.

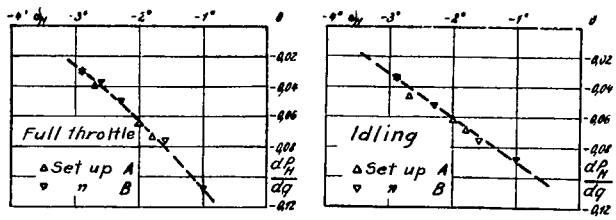

Figure 29.

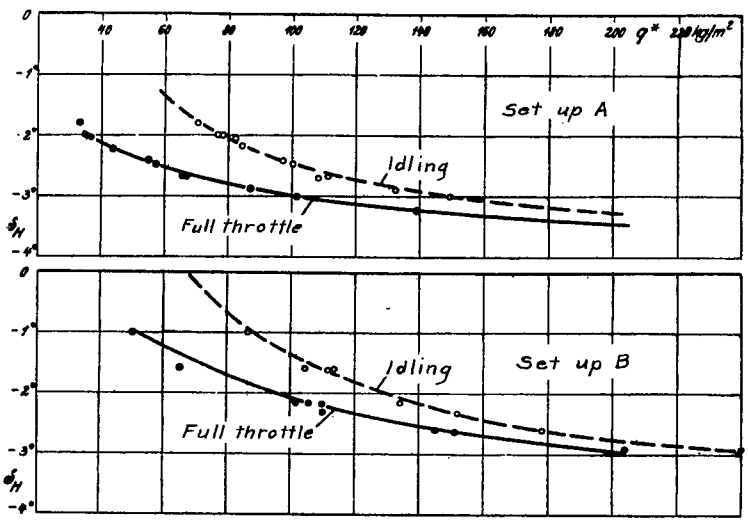

Figure 28.

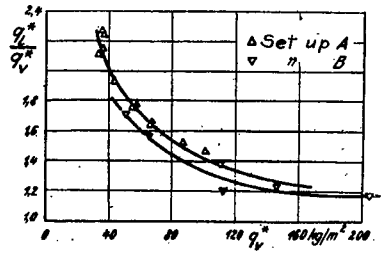

Figure 30.